remote sensing

MDPI

Article

Remote Sensing Intertidal Flats with TerraSAR-X. A SAR Perspective of the Structural Elements of a Tidal Basin for Monitoring the Wadden Sea

Winny Adolph [1,*], Hubert Farke [1], Susanne Lehner [2] and Manfred Ehlers [3]

1 Wadden Sea National Park Authority of Lower Saxony (NLPV), Virchowstr.1, 26382 Wilhelmshaven, Germany; hubert.farke@t-online.de

2 Susanne Lehner, German Aerospace Center (DLR), Remote Sensing Technology Institute (IMF), Oberpfaffenhofen, 82234 Weßling, Germany; Susanne.Lehner@dlr.de

3 Institute for Geoinformatics and Remote Sensing (IGF), University of Osnabrück, Wachsbleiche 27, 49090 Osnabrück, Germany; manfred.ehlers@uos.de

* Correspondence: mail@winny-adolph.de; Tel.: +49-4421-911-155

Received: 1 May 2018; Accepted: 5 July 2018; Published: 7 July 2018

Abstract: Spatial distribution and dynamics of intertidal habitats are integral elements of the Wadden Sea ecosystem, essential for the preservation of ecosystem functions and interlocked with geomorphological processes. Protection and monitoring of the Wadden Sea is mandatory and remote sensing is required to survey the extensive, often inaccessible tidal area. Mainly airborne techniques are carried out for decades. High-resolution satellite-borne sensors now enable new possibilities with satellite synthetic aperture radar (SAR) offering high availability of acquisitions during low water time due to independence from daylight and cloud cover. More than 100 TerraSAR-X images from 2009 to 2016 were used to examine the reproduction of intertidal habitats and macrostructures from the flats south of the island of Norderney and comparative areas in the Lower Saxony Wadden Sea. As a non-specific, generic approach to distinguish various and variable surface types continuously influenced by tidal dynamics, visual analysis was chosen which was supported by extensive in situ data. This technically unsophisticated access enabled us to identify mussel beds, fields of shell-detritus, gully structures, mud fields, and bedforms, the latter detected in the upper flats of every East Frisian island. Based on the high frequency of TerraSAR-X recordings for the Norderney area, a bedform shift was observed in a time-series from 2009 to 2015. For the same period, the development of a mud field with an adjoining depression was traced. Beside seasonal variations of the mud field, the formation of a mussel bed settling in the depression was imaged over the years. This study exemplifies the relevance of TerraSAR-X imagery for Wadden Sea remote sensing. Further development of classification methods for current SAR data together with open access availability should contribute to large-scale surveys of intertidal surface structures of geomorphic or biogenic origin and improve monitoring and long-term ecological research in the Wadden Sea and related tidal areas.

Keywords: synthetic aperture radar; TerraSAR-X; habitat mapping; monitoring; remote sensing; Wadden Sea; mussel beds; intertidal bedforms; tidal gullies

1. Introduction

Tidal flat areas off shallow coasts can be found worldwide. The world's largest coherent intertidal area, the Wadden Sea, is stretching for over 500 km along the North Sea coast of The Netherlands, Germany, and Denmark with a width of up to 20 km. The system of barrier islands, intertidal flats and sandbanks, channels, gullies, and salt marshes forms the transition between the mainland and

the open North Sea. The Wadden Sea is one of the last large-scale and near-natural ecosystems in Central Europe, whose ecological functions are supraregional and of far-reaching importance, e.g., as an indispensable stepping stone for birds migrating on the East Atlantic Flyway. In addition, it also plays an important role in coastal protection. The Wadden Sea is protected by a high national as well as international conservation status and it is listed as UNESCO world heritage site. Regular monitoring of the area is mandatory but complex and expensive because of the large area of rough terrain which is accessible only in tight timeframes due to the changing tides. Therefore, remote sensing techniques are required and aerial mapping and photography (e.g., mussel beds, seagrass meadows, salt marsh vegetation) as well as airborne lidar (light detection and ranging) provide the high resolution needed to determine surface structures of the tidal flats or salt marsh vegetation types. Today they are applied in operational monitoring programs of the Wadden Sea. Aerial photographs have been used in the Lower Saxony Wadden Sea since the 1990s for the monitoring of mussel beds [1–3] and for biotope mapping of the salt marshes [4–6]. Aerial photography and lidar are also used by the responsible authorities for coastal protection (NLWKN, unpublished data). A possible support of the seagrass mappings by aerial photographs was examined by Ref. [7].

Advances in synthetic aperture radar (SAR) technology have enabled a high level of spatial resolution also for satellite-borne sensors implemented by a new class of high-resolution SAR satellites. Since the launch of TerraSAR-X in 2007, followed by TanDEM-X (both X-band), the COSMO-SkyMed satellite constellation (X-band), and Radarsat-2 (C-band), these satellites provide SAR data with resolutions in the scale of meters [8]. The radar satellite Sentinel-1 with a slightly lower resolution (5 m in stripmap mode) has been available since 2014 with open data policy.

With the technical improvements not only offered by the SAR sensors, but also with increasing spatial and/or spectral resolution of electro-optical systems (e.g., Landsat-8, RapidEye, SPOT-4, World-View, or currently, Sentinel-2), the use of satellite data for the protection and management of coastal areas such as the Wadden Sea is becoming increasingly realistic. Against this background, a number of German research projects such as OFEW (2005–2007), DeMarine-1-Environment TP4 (2008–2011), DeMarine-2 SAMOWatt (2012–2015), and WIMO (2011–2015) was conducted to apply high-resolution satellite data for the requirements of monitoring and long-term ecological research in the Wadden Sea; for overviews, see [9–13]. Various authors have demonstrated the value of state-of-the-art satellite data for the exploration of tidal areas [10,11,14–20]. The further development of image classification methods designed for the tidal area has gained pace, for example, regarding the exploitation of polarimetric information from SAR data, whose potential has already been documented by, e.g., Refs. [21–23].

The aim of the present study is to determine the potential of the high-resolution intensity images acquired by TerraSAR-X to identify the distribution and development of the main geomorphological structures and habitats in a whole tidal basin and their dynamics which are of utmost importance for monitoring and long term ecological research but also for the management of the area. In order to recognize as many different surface structures as possible, this study focuses on visual image interpretation, which takes into account backscatter intensity and contrast as well as shapes, patterns, and textures of surface features reflected by the SAR data, but also their configuration or surrounding context. This is of particular importance because the Wadden Sea, characterized by a flat topography, a very dynamic variability, the variety of gradients, transitional zones, and surface structures under the influence of constantly changing water levels and weather conditions, poses great challenges to classification of intertidal surfaces. In this context, visual analysis should provide technically unsophisticated access to as much of the information contained in the SAR data as possible.

Previous knowledge and experience play an important role in the visual interpretation process, with recognition and interpretation running through an iterative process, where both steps heavily rely on one another [24]. That is, context information, such as environmental conditions (acquisition time related to tidal cycle, water level, weather conditions) and processes, field experience, and in situ data, which is difficult to quantify automatically, are essential components flowing into the analysis.

Therefore, in this study, extended field observations partly synchronous to the satellite acquisition are carried out throughout the period of the investigations to validate the image interpretation results. An initial basis of the terrain knowledge was laid during the comprehensive mapping of the main study area as part of the DeMarine-1 project.

TerraSAR-X spotlights and high resolution spotlights proved most suitable to investigate typical intertidal surface structures and habitats such as mussel beds, shell-detritus, gully systems, mud fields, and bedforms which are clearly reproduced and can be drawn from the intensity images by visual analysis. Regarding intertidal bedforms, visual image analysis raised the assumption of bedform movement, therefore the positions of bedform structures in the upper flats of Norderney were further analyzed using the extensive time series of satellite images available for this study. For this purpose, the water-covered bedform troughs were extracted from the TerraSAR-X images using an automated method developed by Ref. [19].

The studies presented here were part of the German research project WIMO (Scientific monitoring concepts for the German Bight) with subproject TP 1.4 (Application of high resolution SAR-data (TerraSar-X) for monitoring of eulittoral surface structures and habitats). In addition, data from the DeMarine-1 and DeMarine-2 projects with the subprojects TP4 (Integration of Optical and SAR Earth Observation Data and in situ Data into Wadden Sea Monitoring) and SAMOWatt (Satellite data for Monitoring in the Wadden Sea) have been included in the investigations.

2. Materials and Methods

2.1. Study Site in the Tidal Flats of Norderney (German Wadden Sea)

The study was carried out in the East Frisian Wadden Sea, which forms the western part of the German North Sea coast between the river Ems and the Weser estuary. Towards the open North Sea, the Wadden Sea is bordered by a chain of barrier islands (Figure 1a). The tidal flats between the island of Norderney and the mainland coast were selected as the main study area. For comparative purposes, surface structures from other parts of the East Frisian Wadden Sea are also included (Figure 1b).

The back-barrier tidal basin of Norderney covers the geomorphic structures and habitats which are frequent and characteristic for Wadden Sea flats: mussel beds, fields of shell detritus, seagrass beds, low lying areas collecting residual waters, a drainage system of channels and gullies and the tidal flats varying in sediment composition from the more sheltered muddy regions near the mainland coast and the watershed to the more exposed sandflats close to the Norderney inlet which connects the tidal basin with the open sea. The different sediment types on the tidal flats and in the subtidal significantly influence the environmental conditions for the organisms living in or on the bottom of the Wadden Sea thus forming habitats with typical species communities. With a mean tidal range of 2.4 m ± 0.7 m [25], the back-barrier tidal basin of Norderney is classified as upper mesotidal according to Ref. [26].

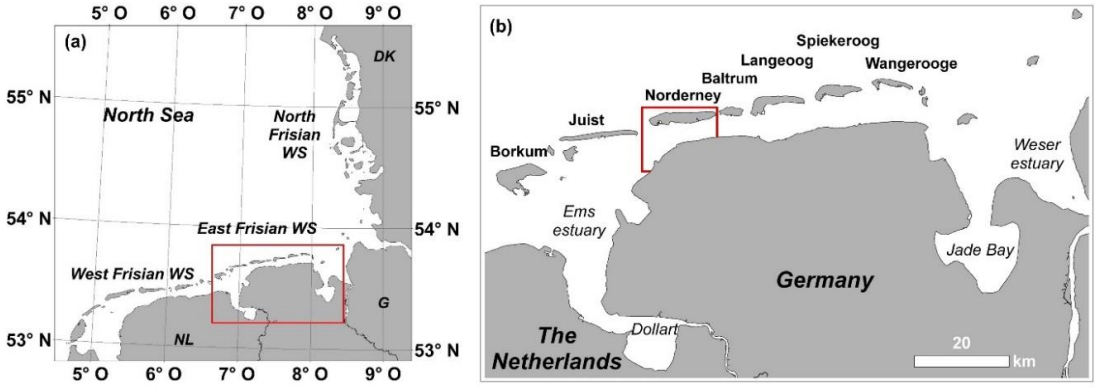

Figure 1. The study area in the German Wadden Sea: (**a**) the Trilateral Wadden Sea in the German Bight; (**b**) the main investigation area located at Norderney in the East Frisian Wadden Sea.

2.2. TerraSAR-X Data Base

SAR data were acquired by the high-frequency (9.6 GHz) X-band sensor of TerraSAR-X with a wavelength of 3.1 cm, operating at 514 km altitude. The data were collected in Spotlight (SL) and High Resolution Spotlight (HRS) mode, which provide ground range resolutions of 1.5–3.5 m [27], few images were taken in stripmap mode with a resolution of 3 m. Since the SAR data should be combined with extensive in situ data and to perform spatio-temporal analyses, Geocoded Ellipsoid Corrected images (GEC) were chosen which can be easily imported into geographic information systems (GIS). To allow acquisition times close to the time of low tide on the one hand, and to obtain a sufficient amount of data on the other hand, SAR data had to be collected at varying orbits and incidence angles. This enabled us to acquire extensive and detailed time series, as well as recordings before and after events such as storm and storm tide or ice drift. From the resulting set of more than 100 TerraSAR-X images available for the years 2009 to 2016, the SAR data documented in this study are listed in Table 1. These images were acquired within the time period 1.5 h before and after low tide and apart from the stripmap image recorded in HH-polarization, the data were taken vertically co-polarized (VV).

Table 1. TerraSAR-X acquisitions used in this study. Image mode: HRS = High Resolution Spotlight, SL = Spotlight, SM = Stripmap, Inc. = Incidence angle, Orbit direction: A = ascending, D = descending, Δ tLT = Acquisition time related to low tide (*positive values*: acquisition at rising tide), Gauge level related to normal height null (NHN), WS, WD = wind speed, wind direction.

Site	Date	Image Mode	Rel. Orbit	Inc. [°]	Orbit Dir.	Δ tLT [min]	Gauge [cm < NHN]	WS [m/s]	WD [°]
Norderney	21/07/2009	HRS	131	20.8	A	63	111 [2]	3.9 [7]	60
Juist/Borkum	05/04/2011	SM	63	37.4	D	9	136 [1]	10.9 [6]	210
Spiekeroog	17/05/2011	SL	40	37.0	A	14	142 [3]	7.6 [8]	270
Norderney	02/06/2011	HRS	116	45.1	A	11	145 [2]	5.4 [7]	360
Norderney	04/06/2011	SL	139	23.3	D	0	160 [2]	5.5 [7]	60
Norderney	16/07/2011	HRS	116	45.1	A	−18	152 [2]	3.2 [7]	160
Norderney	19/07/2011	SL	154	46.6	D	−82	106 [2]	5.5 [7]	190
Norderney	14/10/2011	SL	139	23.6	D	15	174 [2]	3.2 [7]	130
Norderney	10/01/2012	HRS	139	23.5	D	43	116 [2]	3.6 [7]	270
Wangerooge	19/05/2012	SL	116	47.9	A	50	144 [5]	4.8 [8]	30
Baltrum	07/06/2012	SL	63	35.3	D	−52	144 [2]	3.1 [7]	150
Wangerooge	15/10/2012	HRS	40	38.1	A	−2	142 [4]	6.2 [8]	160
Norderney	30/11/2012	SL	63	36.4	D	21	129 [2]	5.4 [7]	10
Norderney	09/06/2013	HRS	131	21.1	A	−23	144 [2]	6.9 [7]	360
Norderney	28/02/2014	HRS	131	21.1	A	63	67 [2]	3.4 [7]	60
Norderney	14/06/2014	HRS	63	36.1	D	46	132 [2]	9.9 [7]	350
Norderney	11/08/2014	HRS	116	45.1	A	6	111 [2]	8.5 [7]	220
Norderney	07/12/2014	HRS	63	36.1	D	56	102 [2]	7.6 [7]	190
Norderney	19/04/2015	HRS	78	54.3	D	40	166 [2]	2.9 [7]	260
Langeoog	21/06/2016	HRS	78	54.2	D	26	105 [2]	2.5 [7]	310

Water level data (source: Federal Waterways and Shipping Administration WSV, provided by Federal Institute for Hydrology BfG) are from the gauges: [1] Borkum Fischerbalje, [2] Norderney Riffgat, [3] Spiekeroog, [4] Wangerooge West, and [5] Wangerooge East. Wind speed and wind direction (source: German Weather Service DWD) are from the weather stations: [6] Borkum, [7] Norderney, and [8] Spiekeroog.

2.3. Image Analysis

The TerraSAR-X data were calibrated to "sigma naught" (σ0), the radar reflectivity per unit area in ground range using ERDAS Imagine (version 2013–2016), to correct for geometry of acquisition cf. [28]. For image interpretation and analysis the intensity images were directly imported into the geographic information system (GIS) of ESRI ArcGIS 10.1 where the data was repetitively verified with geospatial in situ data or compared to monitoring results.

According to initial tests, statistical analysis of backscatter differences such as height, mean value, amplitude, or variance seemed not sufficient for the clear demarcation of most intertidal

surfaces. Therefore, in this study the images are analyzed via visual interpretation integrating i.a. the patterns of internal structures or textures characterizing the surface structures reflected by TerraSAR-X data as well as contextual data including extensive in situ data or weather and gauge level data (cf. Introduction).

2.3.1. Visual Image Analysis

The radar backscatter recorded by the SAR sensor can be considered as a measure of the surface roughness, with smoother surfaces rendered dark in the resulting image and rougher surfaces appearing brighter. Characteristic surface properties of the various structures and habitats in the tidal area therefore lead to corresponding patterns and textures in the radar image. A major difference is seen between water-covered areas and exposed areas such as sediment surfaces and biogenic structures. Although the water surface appears highly variable due to currents, wind, and waves—sometimes in interaction with surface active agents such as biofilms—it can be clearly distinguished from the emerged tidal flats, especially if the edges are markedly distinct. Even from gradual transitions, which are also common in tidal areas, visual references to the surface morphology can be obtained. On the flats, residual water trapped in hollow surface structures helps to detect or identify geomorphic surface characteristics from TerraSAR-X images, such as depressed areas, bedforms, or draining systems. Residual water also contributes to the identification of typical large-scale structures and habitats with specific roughness properties such as mussel beds, fields of shell detritus or mud fields. Associated puddles caught in the humpy sediment surface of a mud field or pools within mussel beds are characteristic features reflected by specific patterns of backscatter in the SAR image.

2.3.2. Digital Image Analysis

Visual image analysis raised the assumption of bedform movement in the upper flats of the island of Norderney, therefore a spatio-temporal analysis of bedform positions was performed using the extensive time series of satellite images collected during this study. To extract relevant markers from the SAR data, bedform positions were determined by detection of the water-covered troughs according to the method proposed by Ref. [19] which is based on textural analysis combined with an unsupervised classification: For comparison with the complete set of TerraSAR-X data, the images were re-sampled at their highest common resolution, a pixel size of 1.25 m. Speckle reduction was performed by edge-preserving Frost and Median filtering and followed by a textural analysis calculating Gray Level Co-occurrence Matrix (GLCM) statistical parameters (variance, homogeneity, and mean) according to Ref. [29]. From the resulting feature images, the water-covered troughs were derived by means of unsupervised ISODATA classification. Image processing was carried out using ERDAS imagine (2013–2015) and ENVI 4.7 software. The classification output was vectorized and imported into ESRI ArcGIS 10.1 for further analysis. The correct assignment of classes was verified by regularly collected in situ data combined with visual interpretation of the SAR images.

2.4. Ground Truth, Monitoring and Environmental Data

Visual image interpretation was performed in conjunction with extensive ground truth data. The background of the terrain knowledge comes from a survey carried out as part of the DeMarine-1 project in 2008/2009 [10,30]. In this context, the tidal areas of Norderney were surveyed according to a comprehensive protocol and photographically documented in a 300 × 300 m grid of stations. In 2014, sections of the grid were revisited for comparison with the 2008/2009 situation. During the current research on the WIMO project, all of the structures described below have been extensively validated by GPS measurements and photo documentation, in part simultaneously with SAR acquisition (cf. Figure 2). Garmin's GPSmap 62s was used for the GPS measurements, the photos were taken with cameras with GPS functionality. Additionally, the bedforms in the upper flats of Norderney were validated by high-precision height measurements recorded by Real Time Kinematic Differential GPS (RTK-DGPS) with a Leica Differential-GPS SR530 and AT 502 antenna type, see [19,20]. Furthermore,

data from the annual mussel monitoring program of the National Park authority in Lower Saxony (NLPV) were used which are obtained by interpretation of aerial photographs. These data are available as shapefiles and indicate the location and areal extent of the intertidal mussel beds of Lower Saxony [31]. Environmental background information included water level data from the gauges at Borkum Fischerbalje, Norderney Riffgat, Spiekeroog, Wangerooge West and Wangerooge East (source: Federal Waterways and Shipping Administration WSV, provided by Federal Institute for Hydrology BfG), as well as wind speed and direction data from the weather stations on Borkum, Norderney and Spiekeroog (source: German Weather Service DWD).

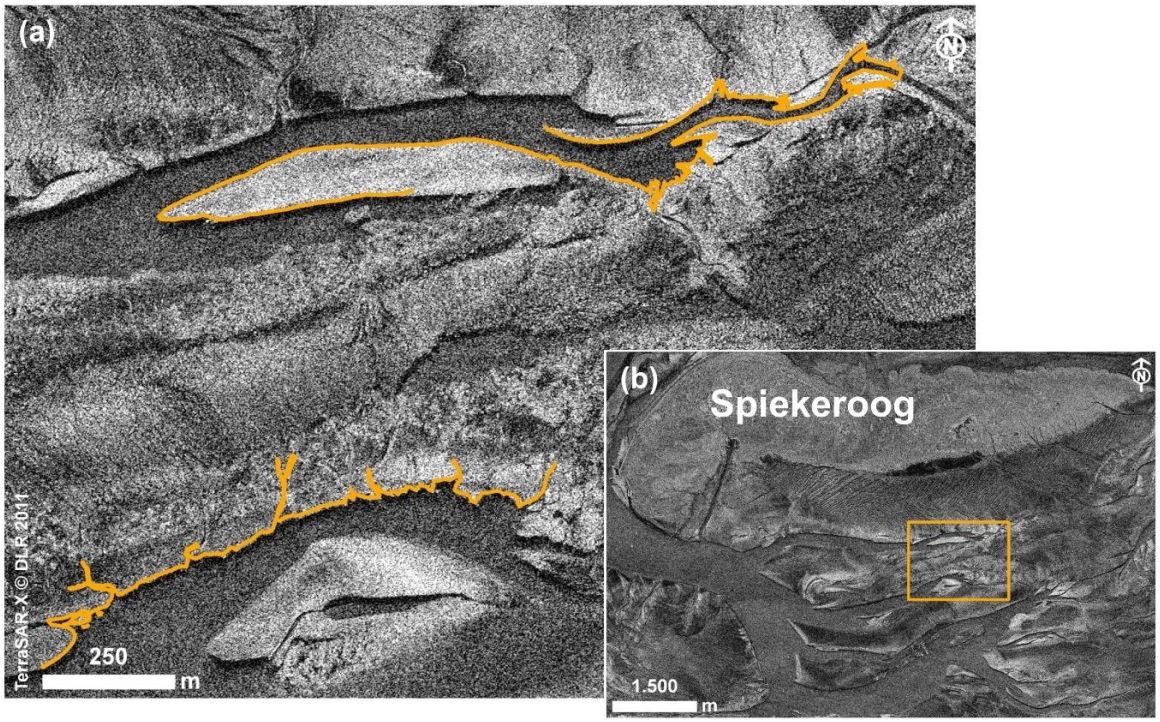

Figure 2. In situ verification of land-water-lines: (**a**) GPS measurement of channel edges synchronous to satellite overflight at 14 min. after low tide (yellow line); (**b**) location of study area (rectangle) in the tidal flats of Spiekeroog (SL of 17/05/2011, ascending orbit).

3. Results

Many characteristic habitats and large-scale surface structures of the tidal flats are clearly reproduced by the TerraSAR-X data. They can be visually identified and analyzed from high-resolution (HRS), spotlight (SL), and, depending on the size of the structure, even in stripmap (SM) images. Figure 3 gives an overview of the main study area, the tidal flats south of the island of Norderney, reproduced by TerraSAR-X. The added in situ photographs illustrate some of the macrostructures imaged by the SAR sensor. Some of them, such as mussel beds or fields of shell detritus, are usually displayed very clearly due to their outstanding surface roughness and specific textures. Edges also, in particular the steeper slopes of channels and gullies or the steeply sloping edges of high sandflats, are clearly shown depending on their orientation relative to the sensor.

Other intertidal structures, however, are specifically reproduced due to the contrasting water and sediment surfaces. Most obvious, water level lines delineate the sub-littoral from the tidal area at low tide or flooded areas from exposed flats in the course of the tides. But also residual water caught in troughs and depressions helps to recognize the relief of tidal flat surfaces indicating structures such as intertidal bedforms, depressed areas, or mud fields.

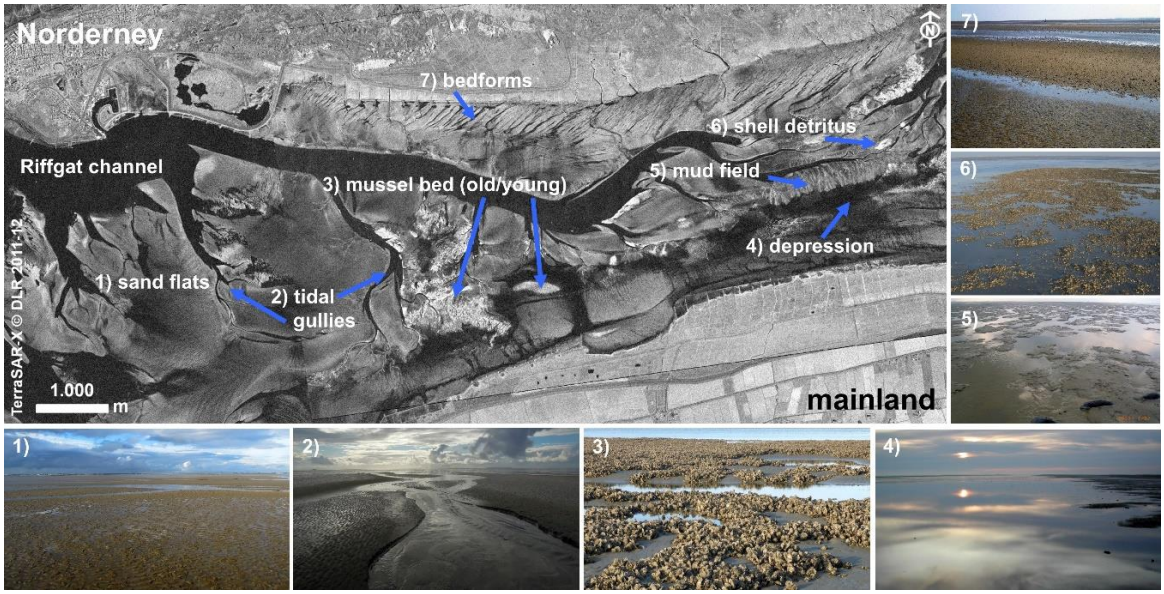

Figure 3. Overview of characteristic habitats and large-scale surface structures of the tidal flats south of Norderney, imaged by TerraSAR-X (02/06/2011 and 30/11/2012, large picture) and the corresponding in situ photographs (small pictures).

3.1. Tidal Channels and Gullies

Twice a day, in the course of the tides, the tidal flats are flooded and drained through the system of tideways, such as channels and gullies. Depending on their position in this system these tideways are exposed to high flow velocities, which especially in sandy environments, causes regular shifts of the edges and leads to highly dynamic channel courses. These tideways can be identified from TerraSAR-X imagery (Figure 4) and over time, also the shifting of their courses or their positional stability. Furthermore, characteristic shapes formed by the branches may provide information about the surrounding sediment.

Channels and gullies are mapped in the TerraSAR-X data depending on their width, the shape of the edges and the surface of the water they contain. In case of water-filled channels, the waterline will mark the edge, whereas for smaller and dry-fallen gullies especially the steep edges eaten into the sediment will be reproduced. The intertidal area shown in Figure 4a exposed to the direct influence of the inlet between the islands of Norderney and Juist open to the North Sea exemplifies morphological development in dynamic tidal areas. TerraSAR-X data from 2009–2012 enables one to observe the shifting of the channel section during that period. Over the entire time, the channel has been relocated by a maximum of over 100 m locally (Figure 4c). The branching arms, by contrast, have remained largely stable. Part of the channel, north of the first branch in the upper part of the image section, is stabilized by an adjoining mussel bed (indicated by internal structures and high backscatter).

By means of visual analysis, the channels are clearly visible in the TerraSAR-X data (Figure 4b,c). However, Figure 4b also illustrates how automatic channel detection may be difficult due to the varying representation of the water surface and to internal patterns e.g., depending on the presence of surface-active agents, weather, or flow conditions at the time of acquisition.

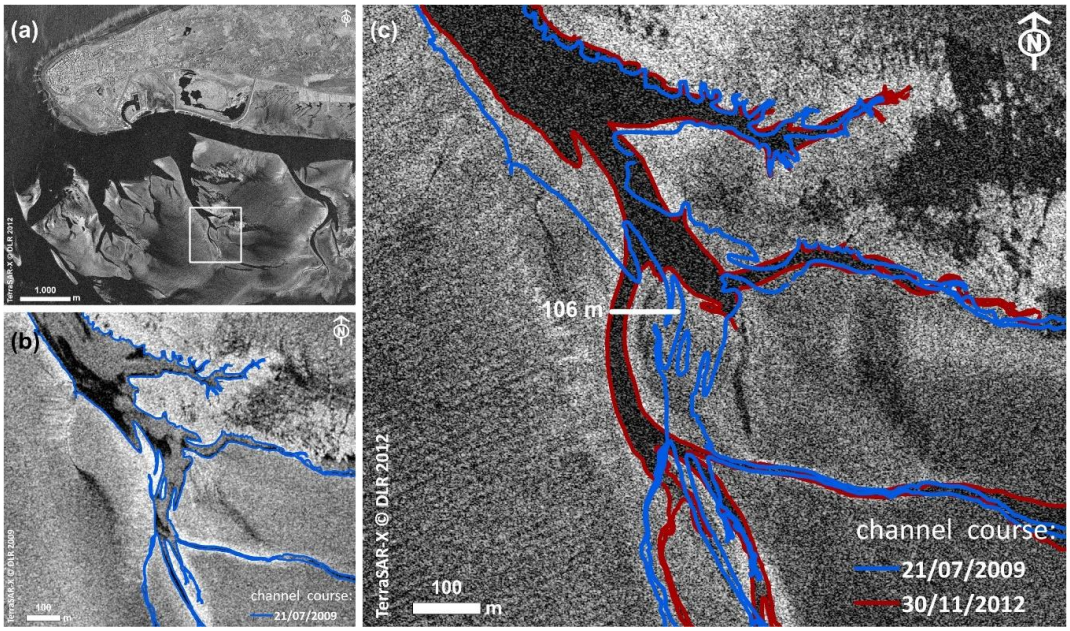

Figure 4. Relocation of tidal channels imaged by TerraSAR-X: (**a**) location of study area (rectangle) in the tidal flats of Norderney (SL of 30/11/2012); (**b**) channel course in 2009 (HRS of 21/07/2009, 111 cm < NHN, ascending orbit); (**c**) shifted channel course in 2012 (red lines) compared to course of 2009 (blue lines) (SL of 30/11/2012, 129 cm < NHN, descending orbit).

3.2. Intertidal Bedforms

3.2.1. Intertidal Bedforms in the Upper Island Flats of the East Frisian Islands

In large areas of the upper back-barrier tidal flats of the East Frisian islands, the sediment surface forms a pattern of periodic crests and troughs thus creating bedform fields of considerable size. The troughs are covered with water throughout the whole time of emergence, therefore the bedforms are clearly reproduced by TerraSAR-X imagery and they can be detected in the whole set of images (acquired from 2009 to 2016) and in the upper island flat of each of the East Frisian islands. In Figure 5, an overview of the bedform fields of the East Frisian islands is given, it shows the bedforms directly adjoining the southern island's shores are generally oriented in a north-easterly direction, but especially in the lower flats also cross-profiles can appear. The dimensions and the exact orientations may vary from island to island.

In the study area at Norderney the bedform positions and their dynamics were examined in detail. The photograph (Figure 6a) gives an impression of their appearance in the field. The bedforms imaged by TerraSAR-X and the vectorized classification result for the water-covered troughs are given in Figure 6b,c.

The results of the survey are described in detail by Ref. [19], who demonstrate that visual trough detection as well as results from unsupervised ISODATA classification of textural parameters from TerraSAR-X data are in good accordance with the in situ measurements of the bedforms. Spatio-temporal GIS-analysis of trough positions extracted from a time-series of TerraSAR-X images then revealed a shifting of the bedforms in an easterly direction during the study period from 2009–2015. This general bedform shift is demonstrated for the years 2012–2015 in Figure 7. The western trough edges are highlighted because in situ measurements as well as TerraSAR-X data reproducing variable states of water-cover indicate an asymmetry of the bedforms leading to steeper western trough edges and smoother eastern edges. Therefore the waterlines of the western edges proved to be a better indicator for the trough positions even with a slightly varying amount of residual water on the exposed flats due to environmental conditions or tidal state.

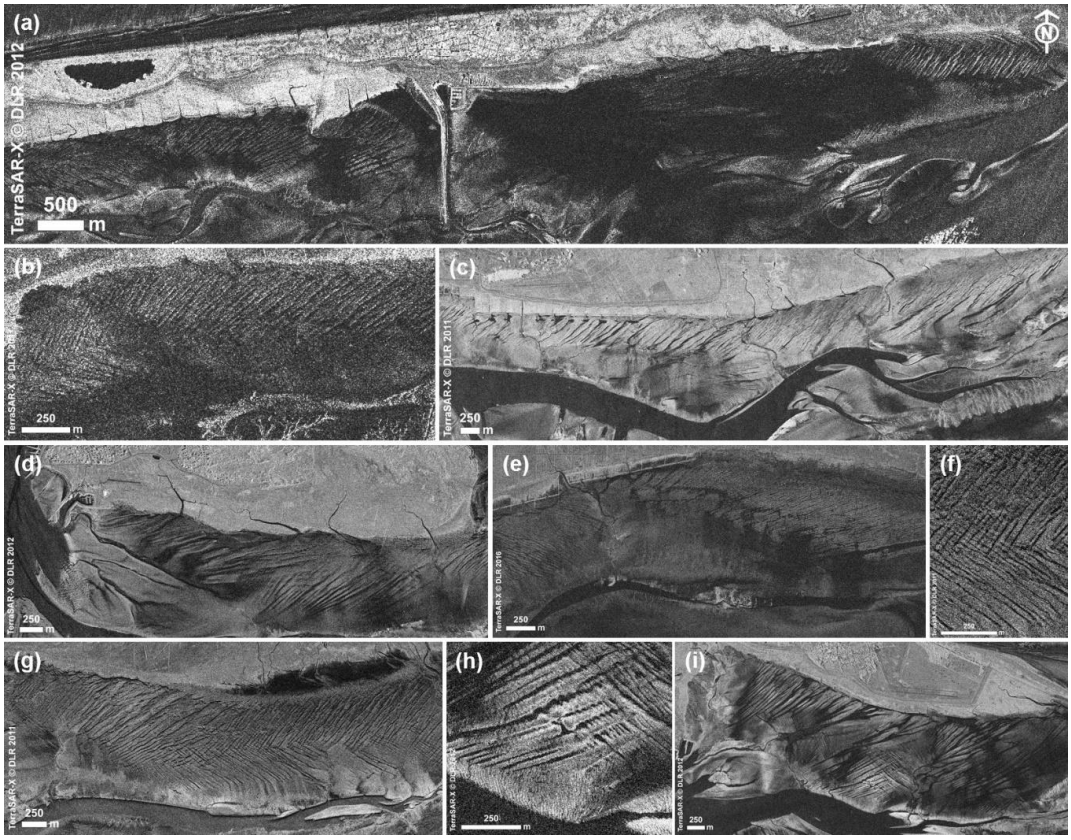

Figure 5. Bedforms in the upper flats of the East Frisian islands imaged by TerraSAR-X: (**a**) Juist (SM of 05/04/2011, desc.); (**b**) Borkum (SM of 05/04/2011, desc.); (**c**) Norderney (HRS of 02/06/2011, asc.); (**d**) Baltrum (SL of 07/06/2012, desc.); (**e**) Langeoog (HRS of 21/06/2016, desc.); (**f**) cross-patterns, detail of (**g**); (**g**) Spiekeroog (SL of 17/05/2011, asc.); (**h**) cross-patterns, detail of (**i**);(**i**) Wangerooge (SL of 15/10/2012, asc.). HRS = High resolution Spotlight, SL = Spotlight, SM = Stripmap acquisition mode of TerraSAR-X, asc. = ascending orbit, desc. = descending orbit.

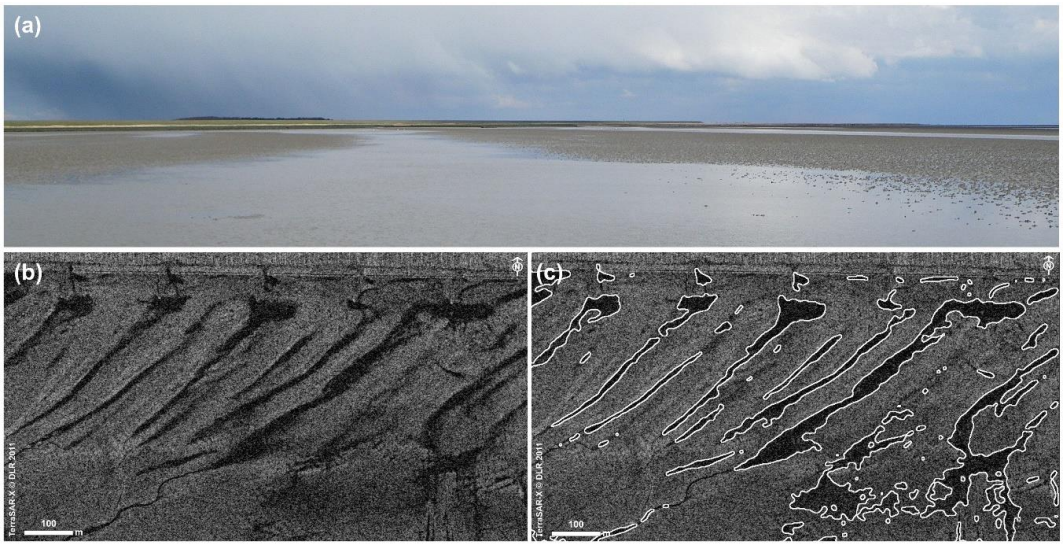

Figure 6. Intertidal bedforms at Norderney: (**a**) photography of intertidal bedforms in the test area (26/03/2014); (**b**) image section: test area in the flats of Norderney (HRS of 02/06/2011, asc.); (**c**) Trough extraction result (white lines) from the same TerraSAR-X data.

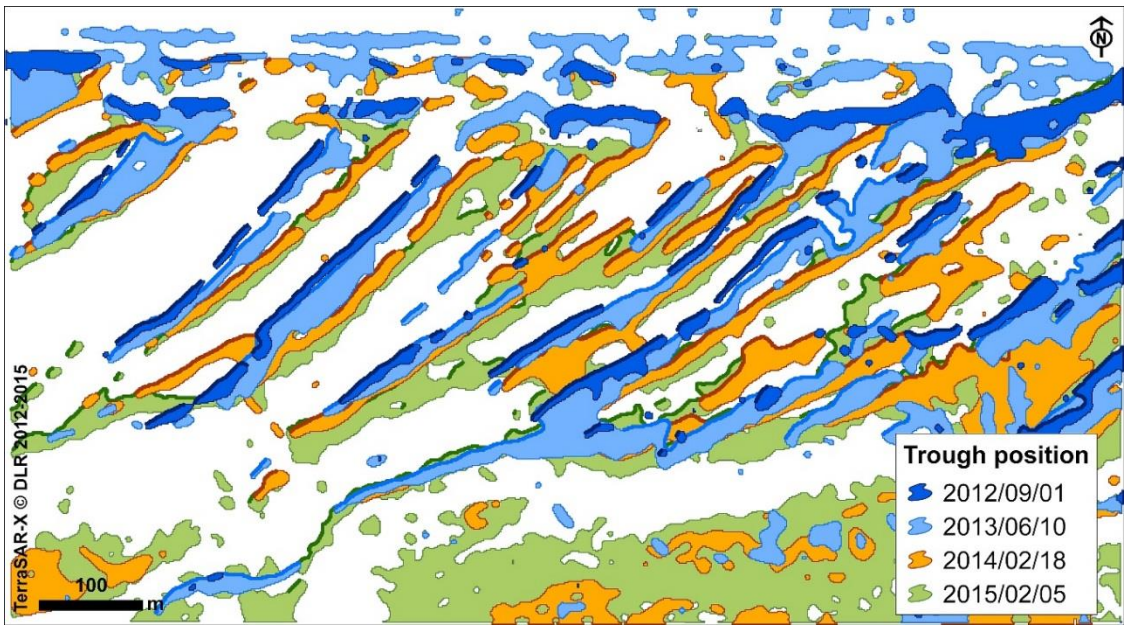

Figure 7. Trough positions extracted from TerraSAR-X images of 2012–2015. Western trough edges are highlighted (reprinted by permission from Springer Nature Terms and Conditions for RightsLink Permissions Springer Customer Service Centre GmbH: Springer Nature, Geo-Marine Letters: Monitoring spatiotemporal trends in intertidal bedforms of the German Wadden Sea in 2009–2015 with TerraSAR-X, including links with sediments and benthic macrofauna, Adolph et al. 2016).

The high frequency of TerraSAR-X data acquisition also enabled us to study the bedform positions in the course of the year and in connection with the effects of storm events. Adolph et al. [19] showed that the trough positions extracted from TerraSAR-X data generally remained stable from late winter to late summer and a shift to the east regularly occurred during winter. The change from the summer to the winter situation in 2013 provides a good insight into the shifting forces. In that year, the troughs kept their positions in every TerraSAR-X acquisition from February to August. However, the TerraSAR-X data from mid-December show a clear bedform shift which is most likely the effect of two very heavy gales in late October and early December with maximum wind speeds exceeding 130 and 120 km/h, respectively [19].

3.2.2. Temporary Surface Structures

Observing the tidal areas by means of TerraSAR-X data, different types of linear structures of the sediment surface were identified. So far, no further investigation of any of these structures has been carried out but similar characteristics were found in TerraSAR-X images of tidal areas throughout the East Frisian Wadden Sea, and also in transition from the tidal to the subtidal areas. In this way, TerraSAR-X imagery opens up new insights into large-scale tidal flat morphology and provides an opportunity to examine its genesis, development, and the significance for the tidal areas.

Southeast of the island of Wangerooge, as an example, in the near-shore area close to the mainland, linear surface structures were detected on a TerraSAR-X image from 2012 and verified in situ. A field of common cockle (*Cerastoderma edule*) apparently stabilized the linear structures and made them both more durable and more conspicuous in the TerraSAR-X data. Additionally, the elevated ridges of the sediment and cockle surface were covered by green algae, which contributed to the clear picture (Figure 8). In situ observations in 2016 have shown that in the meantime, the cockle field had been occupied by blue mussels (*Mytilus edulis*) and turned into a patchy mussel bed.

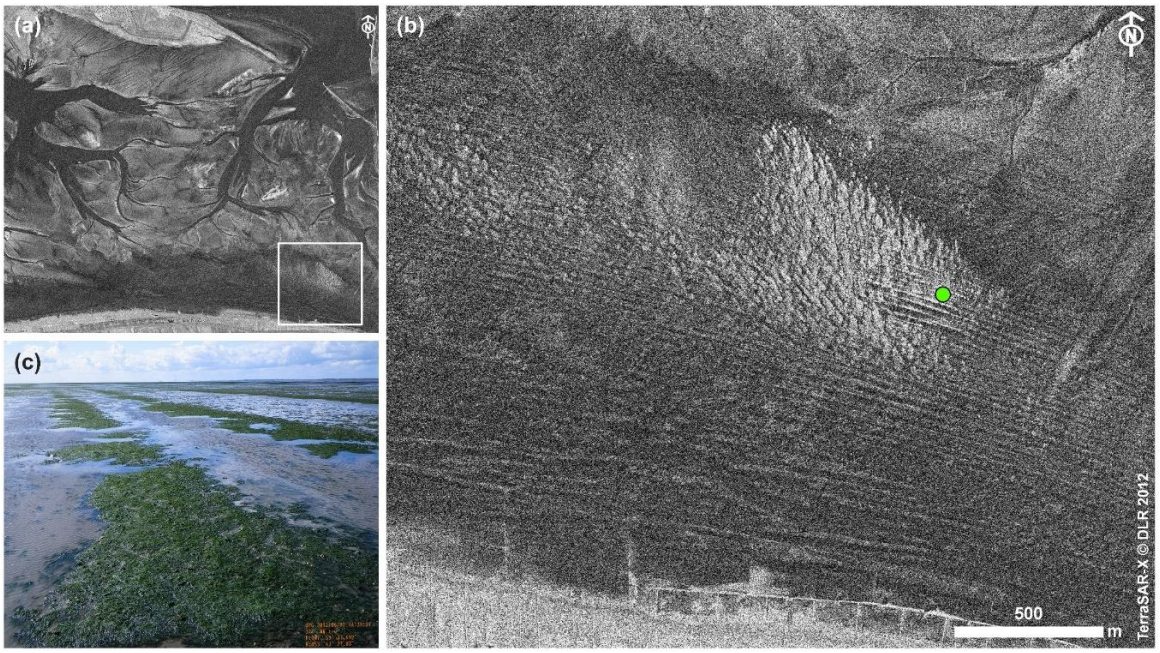

Figure 8. Temporary linear surface structures in the tidal area south of Wangerooge: (**a**) Tidal flats between the island of Wangerooge and the mainland coast, rectangle marks image Section b (SL of 19/05/2012, asc.); (**b**) linear surface structures within and in the surroundings of a cockle field (*C. edule*), point marks position of photographer; (**c**) photography of surface structures (02/06/2012).

3.3. Mud Field

The large mud field close to the watershed of the tidal flats beneath the island of Norderney extends over ca. 1.8 km along the Riffgat channel (see Figure 9) with a width of 300–400 m. On the wavy to humpy sediment surface, water puddles formed between the muddy humps resulting in a characteristic pattern (see Figure 9e), leading to a relatively high backscatter in the TerraSAR-X data. In addition, the mud field is traversed by a dense network of highly branched gully structures which drain the water from the adjacent depression in the south of the mud field to the channel in the north. These properties lead to a specific reproduction of the mud field in the TerraSAR-X images characterized by a high backscatter and the recognizable texture of the many gully structures (see Figure 9b). The contrast with the Riffgat channel and the water covering the area of the depression also facilitate to determine the contours of this mud field. In situ the southern edge of the mud field is clearly marked by the finely branched gullies originating from the water-covered depression. Here, the surface of the muddy deposits stands out from the more solid, smoother sediment surface of the depressed area (see Figure 9c,d). Therefore, GPS measurements of the mud field's edge carried out in summer 2011 (27/07/2011) show very good agreement with the contours reproduced by the TerraSAR-X acquisition recorded within a short time frame (16/07/2011). In Figure 9b, the yellow line represents the GPS measurement.

Figure 9. Large mud field in the tidal area of Norderney: (**a**) location of the mud field close to the watershed, marked by oval line (HRS of 02/06/2011, asc.); (**b**) GPS measurement of mud field's edge taken on 27/07/2011 (yellow line) compared to TerraSAR-X HRS of 16/07/2011, asc.; (**c**) photography along the mud field's edge (27/07/2011); (**d**) gully delta at the mud field's edge (27/07/2011); (**e**) humpy mud field surface with water puddles (27/07/2011).

Seasonal Aspects

In situ studies show variations in the surface form of the mud field. Extent and height of the muddy humps vary as well as their shape, which can be smooth and wavy or in contrast have steep erosive edges. These variations may occur locally, e.g., the silt surface always tends to be smoother on the edge of the mud field towards the depression. Overall, however, the field surveys showed that the mud field surface was more pronounced during the calmer season of the year (usually the summer) than after the stormy time of winter. When GPS-measuring the mud field's edge in summer 2011 (27/07/2011), the mud deposits clearly stood out from the depressed area covered with water. Thus, the boundary of the mud field was obvious and also well defined by the waterline (see Figure 9b,c). In the following January (17/01/2012), after two storms had passed through in the first days of the month (03–06/01/2012), a much more gradual transition was observed from the depression to the mud field. While the gully deltas where still in place, the smooth, slightly wavy surface of the silt accumulation began to emerge only gradually from the lower area, just beyond the ends of the gully deltas.

In fact, regarding the mud field over several years (2011–2015) in the TerraSAR-X data, seasonal changes are observed. During summer, the mud field surface is displayed in full width with high backscatter, in winter, however, the area of high backscattering retreats towards the Riffgat channel. The internal gully structures, on the other hand, remain visible throughout the year, across the entire width from channel to depression. This can be seen in Figure 10a–d showing the reproduction of the mud field in TerraSAR-X acquisitions from summer 2013, the following winter (02/2014) and the next summer (06/14) and winter (12/2014).

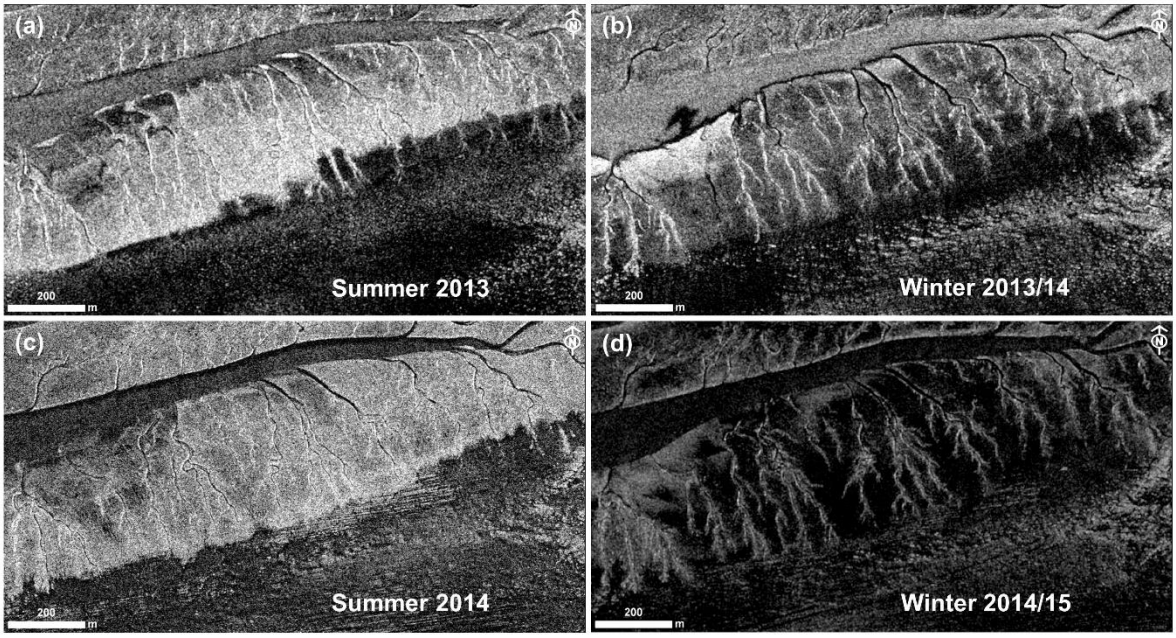

Figure 10. Seasonal aspects of the large mud field close to the watershed of the tidal area of Norderney reproduced by TerraSAR-X HRS acquisitions, VV polarised, ©DLR: (**a**) 09/06/2013, orbit 131, asc., 144 cm < NHN; (**b**) 28/02/2014, orbit 131, 67 cm < NHN; (**c**) 14/06/2014, orbit 63, desc., 132 cm < NHN; (**d**) 07/12/2014, orbit 63, 102 cm < NHN.

The formation of similar mud fields between tidal channels or expanded gully deltas and low-lying, often water-covered flat areas (depressions) with a network of gullies connecting both across the mud field, can also be seen in SAR images covering the tidal areas of other East Frisian islands.

3.4. Mussel Beds

Intertidal settlements of blue mussels (*M. edulis*) associated with Pacific oysters (*Crassostrea gigas*) form solid structures sticking out above the sediment surface. These biogenic structures are characterized by a high surface roughness caused by the mussels and by the larger Pacific oysters often growing upright. They are reflected with high backscatter in the SAR images and the varying forms of appearance in which mussel beds occur in situ are also reproduced by the TerraSAR-X data: Young beds that have settled during an actual spat fall are relatively homogeneously occupied by mussels or by homogeneously distributed smaller patches. Over the years, a typical structure of mature beds develops, in which more or less elevated areas covered by mussels form an irregular pattern with open interspaces. This is reflected in the TerraSAR-X data accordingly, with young beds showing homogenous backscatter, while old mussel beds have characteristic internal structures (Figure 11a). In most cases the mussel beds reflected by TerraSAR-X are in good agreement with field observations or with the monitoring results currently obtained from aerial photographs. This is exemplified in Figure 11b, where the yellow line represents the monitoring result from the year of the TerraSAR-X acquisition.

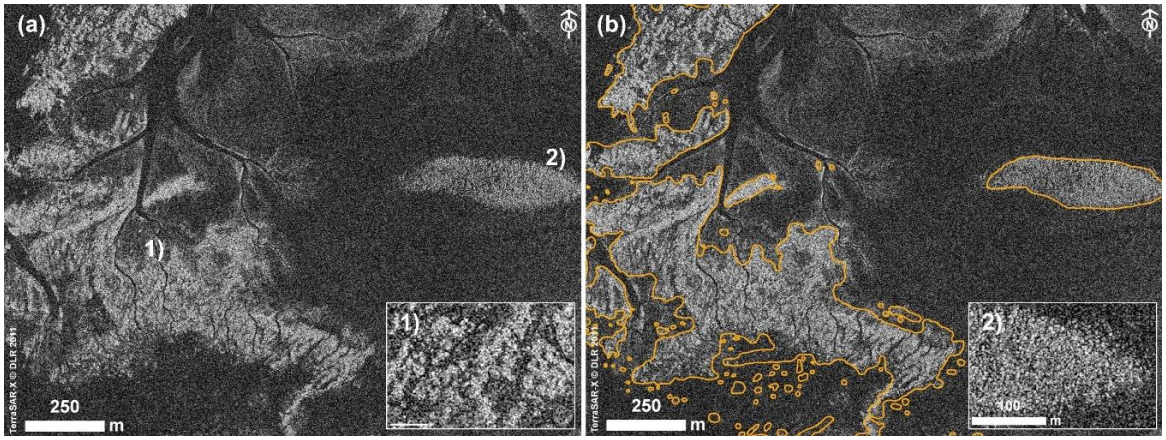

Figure 11. Mussel beds in the central area of the tidal flats south of Norderney imaged by TerraSAR-X (SL of 19/07/2011, desc.): (**a**) established old mussel bed (1) and young mussel bed (2); (**b**) yellow line represents monitoring result from aerial photography interpretation (2011).

3.5. Tidal Flat Dynamics Imaged by TerraSAR-X

The tidal area close to the watershed of the Norderney basin between the eastern Riffgat channel and the mainland coast may serve as an example to demonstrate both the stability and the variability of tidal areas and their reproduction in the TerraSAR-X data. A time series of TerraSAR-X images shows the developments taking place in this area from 2009–2015 (Figure 12). The branches of the Riffgat channel, at the top of the picture, do not change their courses during this period. Likewise, the large mud field (Figure 12, Region 1) remains as such, only the shape of the southern edge, constituting the boundary to the adjacent depression, changes slightly. The gully structures within the mud field remain essentially the same, even if displacements occur in the course of the smaller branches. Since the TerraSAR-X data were recorded in April to July, the mud field is shown in the aspect of the calmer season in each of the four SAR acquisitions. Compared to 2009, the area increased slightly in 2011, 2014, and 2015.

Most obvious in the SAR data, however, is the development of mussel beds in the low lying area south of the mud field (Figure 12, Region 2-4): in the field surveys of 2008/2009, this area proved to be a depression with open sediment surface, often water-covered, and in wide areas densely populated by common cockles (*C. edule*) and the polychaete worm sand mason (*Lanice conchilega*). Sand masons build tubes protruding up to a few centimeters above the sediment surface which leads to an increased roughness, particularly when they break through the surface of shallow water covering the flats (Figure 12a, Region 4, see also photography in Figure 12a). Just like the shell detritus of cockles (cf. chap. 3.2), sand masons can serve as a substrate for the settlement of blue mussels. In 2011, the first mussel settlement in this location was reproduced in the TerraSAR-X image (Figure 12b, Region 4), and in the data from 2014, the mussel bed with its internal structures is already well recognizable as such (Figure 12c, Region 4, photography in Figure 12c). The typical pattern of an established mussel bed can be seen here in 2015 (Figure 12b–d). Southwest of the mud field however, a mussel bed with open structures developed from 2009 to 2011, which in the following years recedes and confines to a few central bed structures in 2014/2015 (Figure 12, Region 3).

In effect, the area of the extensive depression clearly discernible in 2008–2011, has narrowed until 2015. It has been taken up, in particular, by scattered mussel settlements but also by accumulations of muddy sediment, partly forming temporary linear structures (Figure 12c,d, Region 2) which are visible at the mud field's edge in 2014 and throughout the area of the formerly water covered depression. These may be due to the unusually turbulent summer season of that year [32,33].

South of the mussel bed in Region 3, higher backscatter is visible especially in the 2014 acquisitions (Figure 12c). From the field surveys it is known that, in this area, fields of seagrass patches occur.

Seagrass itself was not detected in the TerraSAR-X data according to this study, as it lies flat on the sediment at low tide and is characterized mainly by its spectral features. In some cases, though, the seagrass vegetation leads to the formation of elevated surface structures, which are reflected in the SAR data.

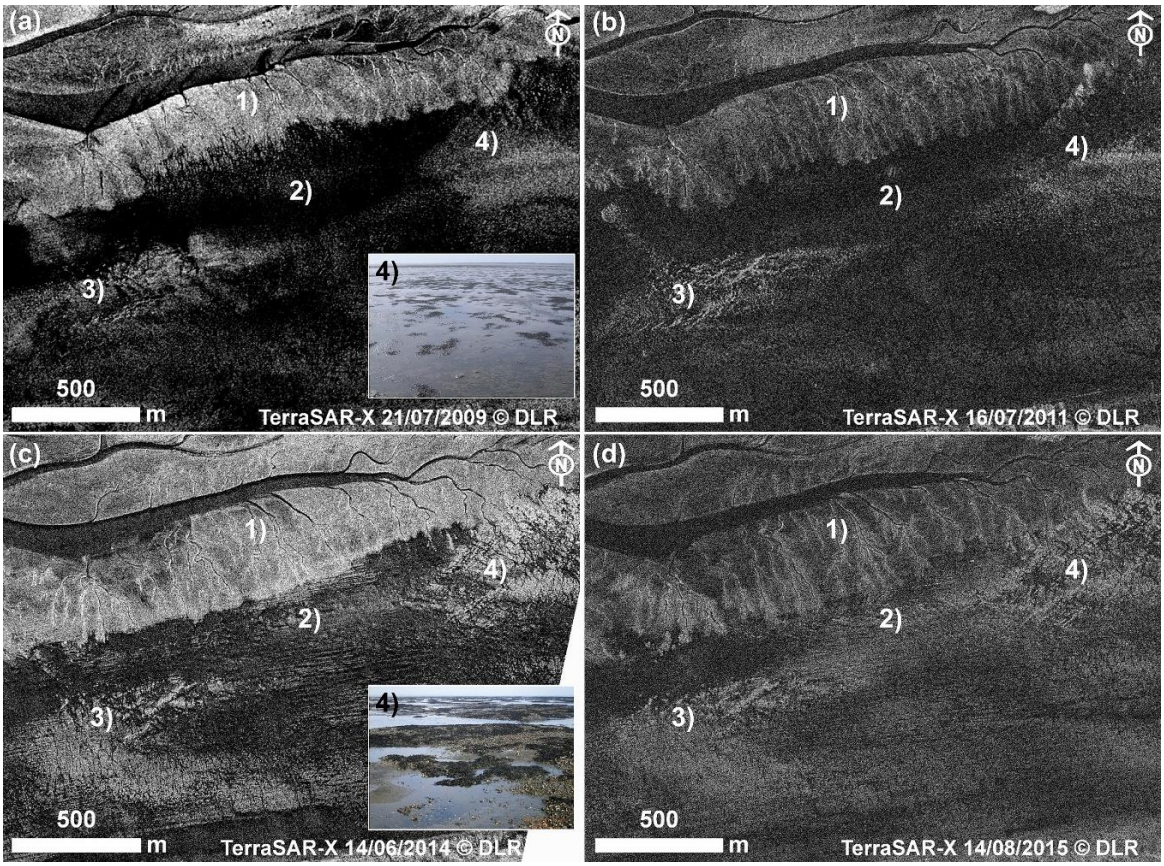

Figure 12. Time series 2009–2015 of tidal area imaged by TerraSAR-X, HRS: (**a**) 21/07/2009, asc., 111 cm < NHN and photograph of 14/07/2008; (**b**) 16/07/2011, asc., 152 cm < NHN; (**c**) 14/06/2014, desc., 132 cm < NHN and photograph of 17/10/2014; (**d**) 19/04/2015, desc., 166 cm < NHN. (1) mud flat; (2) depression; (3) area of patchy mussel bed; (4) area of solid mussel bed.

In summary, certain habitats and structures such as the mud field, mussel bed, or the water-covered depression are clearly recognizable in the TerraSAR-X data due to typical characteristics and patterns. Intermediate states of developments or vague surface structures, on the other hand, can only be identified through field observations or context knowledge. This applies, for example, to the extensive fields of sand mason, which can be recognized at the appropriate level of residual water due to the disturbance of the smooth water surface, to scattered young mussel settlements and oyster scree scattered by winter storms, or to the surface structures sometimes generated by seagrasses.

For monitoring, often it is sufficient to carry out a correct identification of a structure in situ once, to determine its characteristics and boundaries. Further development can then be monitored via TerraSAR-X data.

4. Discussion

The results of the present study show the great potential of satellite SAR data to contribute to the monitoring of the tidal Wadden Sea area. Visual image interpretation of TerraSAR-X data combined with extensive in situ data enable the detection and observation of various large-scale surface structures and characteristic habitats. This is to be emphasized as the smooth and dynamic relief of the Wadden

Sea, influenced by variable water levels and weather conditions, places great demands on classification methods in general.

4.1. Geometry of Acquisition

In general, using different geometries of acquisition, different angles of incidence, and ascending and descending orbit directions, we found that the reproduction of surface structures indicated or amplified by the contrast of sediment and water surfaces is relatively insensitive to geometry of acquisition when making use of visual image interpretation. The same holds for habitats with an extensive three-dimensional surface roughness, such as mussel beds, mud fields, and fields of shell detritus which can be visually identified by their specific patterns and textures under the differing geometries we used.

However, we found some variations in the characteristics of the TerraSAR-X images are due to varying incidence angles of the geometry of acquisition. In near range, that is at small incidence angles <24° (relative orbits 131, 139), the images show sharp contrasts and widespread high backscatter. Therefore, strongly scattering structures are not well demarcated from each other: Mussel beds, humpy mud fields with a dense network of gullies, sediment surfaces roughened by sandworm (*Arenicola marina*) heaps, and steep sandy slopes (depending on exposition in relation to sensor, orbit direction) are displayed similarly brightly which makes the differentiation of these surfaces more difficult. Furthermore, in mussel beds, internal structures are less recognizable. However, when surrounded by smooth surfaces, e.g., smooth water cover, these scatterers stand out sharply. Any roughness of the water surface, on the other hand, is also highlighted and eddies and currents can clearly be seen when biofilms or other surface-active agents are present. As backscatter values of the flooded areas can be quite high, they often exceed those of smooth intertidal surfaces.

With incidence angles of 30–40° (rel. orbits 40, 63), the water surface becomes more uniform and scatters less, the images are less sharp in contrast and more differentiated in the backscatter values. Mussel beds and other structures with high backscatter are better distinguished from each other and from rougher surroundings.

Increasing incidence angles of 40–47° (rel. orbits 116, 154), amplify further differentiation of backscatter intensities. Mussel beds, for example, stand out more clearly from their surroundings, from other rougher surfaces, or from steep edges with high backscatter, which is also due to the fact that the internal structures are better recognizable. Fine linear structures of the sediment surfaces are clearly visible.

All of this is reinforced with incidence angles above 50° (rel. orbits 25, 78). Mussel beds are clearly recognizable. However, gradual transitions are now displayed very fluently and demarcations are therefore less obvious. Under good environmental conditions, i.e., with well drained flats, fine surface structures are clearly visible (e.g., linear structures).

In summary, for most intertidal surface types acquisitions at incidence angles between 30–47° therefore are most suitable. For specific questions smaller or higher incidences can be useful.

4.2. Environmental Influences—Water Cover

An essential aspect in the interpretation of SAR images from tidal areas is the varying presence of water. Apart from the tidal cycle, the water regime is influenced by external conditions affecting tidal water level and, to a lesser extent, also residual water remaining on the flats. Therefore, knowledge of weather and environmental conditions at the time of recording or in the time before may be essential for image analysis. Time of exposure, wind speed and direction, as well as spring/neap tides affect the water coverage in the area but they may also influence the roughness of water and sediment surfaces or sediment moisture. Hence, the same area may appear partly different in SAR acquisitions taken at different times. In general, the flats are better drained after low tide compared to the time of falling tide, even at the same gauge level. Such effects should be taken into account as well as knowledge about general processes and phenomena occurring in tidal areas.

As an example, the appearance of tidal channels, creeks, and gullies reproduced in SAR images is heavily dependent on water level as soon as the water reaches the tideway's edges or goes beyond. Therefore, changes in water level due to weather conditions or even wind-drift may have an effect especially on the gently rising slip-off slopes in contrast to the steep edges of the eroding banks, whose positions will not be markedly affected even for larger variations of the water levels. Thus, to observe and compare the courses of channels and gullies, they should on the one hand be imaged close to maximum drained stage, and on the other hand the steep eroding banks should be used as markers. The same applies when determining migration rates for bedforms in the upper island flats, whose slopes have been found to be slightly asymmetrical [19]. Conversely, in the case of multi-temporal acquisitions, the magnitude of changes in the water level lines would indicate the slope inclination.

On the whole, the SAR data used in this study not only image the channel network and drainage system in tidal areas but they also provide a valuable source of insight into surface morphology of tidal flats mapped due to accumulation of residual water on the exposed flats. Such are the distribution of depressed areas indicated by frequent water coverage or troughs marking bedforms of the sediment surface.

4.3. Visual Analysis and Classification

Overall, the visual approach proved generic enough to provide an overview of most elements structuring the main research area at Norderney by taking into account not only statistical parameters such as backscatter intensity and contrast, but also shapes, sizes, patterns, and textures of surface features reflected by the SAR data, as well as their spatial distribution and surroundings. Especially patterns, texture, and context information proved to have a great significance for the image interpretation. The importance of contextual information—site and time specific—in SAR image interpretation is also emphasized by Ref. [34] who studied the effects of environmental factors and natural processes on radar backscattering in the Korean tidal areas.

Although successful application of TerraSAR-X images is shown, the results also indicate problem zones and variations with the risk of misinterpretation. Areas with no clearly distinctive features or with broad transition zones between habitats may demonstrate the limits of exact demarcation. Mussel beds can exemplify both clearly identifiable areas and problem zones, which will be discussed in the following.

Mussel beds are particularly well recognized by their specific internal structures of beds and interspaces, which also allow a certain understanding of their maturity and compactness. Still, due to variability in the appearance of habitats and structures, misinterpretation can occur, e.g., with shell detritus. Mostly, fields of shell detritus are easy to distinguish from mussel beds, because they lack the characteristic internal structures. However, for young mussel beds or very densely covered areas of mussel beds, internal structures may be similar. In these cases, supplementary in situ data is necessary for correct interpretation of the SAR data. Likewise, steeply sloping edges of high sand flats exposed to the sensor could be mistaken for dense beds of mussels or shell detritus, although these are often recognizable from their location, or from comparison with acquisitions of a different recording geometry. In case of doubt, the structure should be clarified on site. Surfaces that have been identified and verified can then be tracked over time in the SAR data with little effort. Or they can also be identified in other places with this acquired knowledge.

The sole visual analysis of the TerraSAR-X images may also reach its limits when it comes to determining the exact demarcation of surfaces which directly merge into each other with flowing transitions e.g., where mussel beds are directly surrounded by humpy mud flats or fields of shell detritus that extend far beyond the mussel bed and represent their own habitats. In such cases, again, field observations are needed. Preferably, additional distinguishing characteristics are to be found to design a specific classification method, for example, by exploiting the polarized information of the SAR data. Various authors have shown the additional potential of multi-polarization SAR imagery for the detection of bivalve beds, using fully polarimetric e.g., [35,36] or dual-copolarized SAR data [37,38].

Wang et al. [22] discriminated bivalve beds from the surrounding bare sediments through polarimetric decomposition based on dual-copolarized SAR data. Further research is needed to investigate to what extent polarimetric information can be used for the detection of other surface types in the tidal area. Geng et al. [21] identified different surface cover types (i.e., seawater, mud flats, and aquaculture algae farms) through polarimetric decomposition, and Ref [39], and recently Ref [23] pointed to the potential of fully polarimetric interpretation of SAR imagery for classification purposes in tidal areas.

Gade et al. [23] found evidence of mapping characteristics of seagrass beds in SAR data from the Schleswig-Holstein Wadden Sea, whereas in the present study, no general detection of seagrass is proven. In some cases, areas of which seagrass vegetation is known from the field surveys, were characterized by diffusely elevated backscatter values, which may be due to elevated structures of the sediment surface induced by the seagrass cover. Comparative areas vegetated by seagrass, however, could be completely inconspicuous in the SAR data. However, the seagrass stocks in the Lower Saxony Wadden Sea are smaller and of significantly lower density than those in the Schleswig-Holstein Wadden Sea. For these reasons, recognition of seagrass was not pursued in this study. Still, seagrass is a parameter required for Wadden Sea monitoring. For test areas in the Schleswig-Holstein Wadden Sea, Ref. [11] showed that seagrass meadows can be classified based on optical satellite data with a high degree of detail. At present, electro-optical sensors seem to be essential for the detection of seagrass—respectively of vegetated areas—but merging with SAR data could also include surface roughness information. If it is proven that seagrass meadows produce characteristic surface structures reflected by the radar return, this could facilitate their differentiation from green algae or diatoms.

Sediment distribution on tidal flats is another information that would be important for monitoring, but could not be directly obtained from the SAR data by visual interpretation. In some cases indirect detection methods are conceivable, e.g., for mud fields, which are characterized by a humpy surface with puddles and dense gully structures. Also channel network features i.e., the meandering patterns, density and complexity of creeks and gullies and their branches provide, among others, information about the surrounding sediment. The authors of Refs. [40,41], who extracted the geometric information of tidal channels from aerial photography as well as Ref. [42], using electro-optical satellite data (KOMPSAT-2), found lower tidal channel density in areas of higher sand percentage, while complex and dendritic channel patterns were found in mud flat areas. Regarding movement of sediment, Ref. [43] applied the waterline technique to satellite SAR to form a Digital Elevation Model (DEM) of the intertidal zone of Morecambe Bay, U.K. for measurement of long-term morphological change in tidal flat areas. Automated waterline extraction from SAR imagery is used by Ref. [44] for determination of changes in coastal outlines.

The present study shows that visual interpretation of SAR imagery has its own value in support of monitoring and questions of ecological or morphological research in tidal areas. It provides technically unsophisticated access to remote sensing information about characteristic surface structures which can be used by nature protection managers or researches of various disciplines. As a first analysis approach, visual interpretation can also indicate the potential of the satellite SAR data for further investigation and thus may provide pointers for the development of automatable classification methods with regard to monitoring requirements. Currently, Sentinel-1 is providing an increasing base of SAR data available with open and free access which can be screened for monitoring and research for the Wadden Sea.

4.4. Contribution of Satellite SAR for Future Monitoring of Tidal Flats

The regular recording of position, area, and status of characteristic spatial structures in defined time intervals is an indispensable condition for monitoring tidal flat areas such as the Wadden Sea. Monitoring this area has to integrate differing requirements which cannot be provided by a single sensor system. Therefore, a spatially and temporally differentiated monitoring concept combining the benefits of different sensor classes has to be developed. This study has shown that particularly habitats and geomorphic structures characterized by their surface roughness combined with specific textures and patterns are clearly recognizable in TerraSAR-X acquisitions. Other surface structures are virtually

marked by residual water, which is an outstanding advantage of this sensor technology. Because of the high temporal availability, SAR data are also predestined to cover periods between sumptuous in situ campaigns, expensive recordings such as lidar scans, or electro-optical acquisitions dependent on daylight and weather. Thus, continuity in the tracking of dynamic structures can be ensured or new events can be discovered in a timely manner by the SAR sensors.

Another approach to meet the monitoring requirements is to directly fuse data from different sensor systems to leverage their respective benefits concerning areal coverage, spatial and temporal resolution, sensitivity, and geometric accuracy while also taking into account financial aspects. In this regard, the advances in satellite technology and the open data policy for imagery from an increasing number of sensors, such as recently the sentinel satellites from the ESA Copernicus program, has already promoted the development of image classification methods. Against the background of the different sensor properties, the combination of different SAR sensors as well as SAR and optical sensors has been examined to refine the differentiation between scatterers or to obtain high-resolution multispectral images e.g., [45–48]. For tidal areas, e.g., Ref. [49] used information from both space-borne microwave (SAR) and optical/shortwave infrared remote sensing to determine sediment grain-size of tidal flats in the Westerschelde, and Ref. [50] investigated the use of multi-frequency SAR data for sediment classification and for the detection of bivalve beds. Results from the DeMarine projects [10,11,14] and the WIMO project [15,17,20] have also shown that a combination of high spatial resolution SAR data and specific spectral resolution (specific wavelengths) benefits the classification of intertidal habitats. New algorithms and procedures in the area of neural network deep learning [51,52] may also bring advances in information extraction from satellite data.

So, to develop operational methods that harness satellite-based remote sensing data for Wadden Sea monitoring and meet the requirements of monitoring obligations from national and international legislation, the advantages of various sensor classes and methods of information extraction will have to be combined. Regarding the exponential growth of technology and methods of information extraction, interdisciplinary research as well as collaboration of nature protection managers with experts in electro-optical and SAR remote sensing will be absolutely beneficial.

5. Conclusions

- High-resolution SAR data as recorded by TerraSAR-X enables identification of essential geomorphic surface structures and habitats of the Wadden Sea ecosystem and their dynamics.
- Independence of SAR sensors from daylight and weather and a high repetition rate (11 days for TerraSAR-X) offer high temporal availability of data and allow to record long-term developments, short-term (e.g., seasonal) developments, and also event effects (e.g., storms, human intervention).
- Even in the spotlight modes providing highest spatial resolution, the footprint of one acquisition covers about the area of a tidal basin. This allows one to determine the status, size, and distribution of the intertidal macrostructures and habitats of a whole sub-unit of the Wadden Sea ecosystem.
- Visual interpretation of TerraSAR-X data combined with context information such as ground truth, monitoring results, or data on environmental conditions, both integrated in a GIS, proved to be a technically unsophisticated access to the information contained in the SAR data. As a first analysis approach, it can also provide basics for the further development of automatable classification methods.
- High-resolution SAR sensors can contribute relevant data for remote sensing the Wadden Sea. For future Wadden Sea monitoring or long-term ecological research, the combination or fusion of appropriate sensor data (e.g., SAR, multi-spectral data) is promising to significantly expand the interpretation options of advanced satellite-borne remote sensing techniques and to develop automated classification methods.
- In this study, the integration of diverse spatial data (such as large-scale remote sensing data and local sampling data) in a GIS has emerged as an essential component assisting the visual analysis. Beyond that, in a broader context, GIS allow to merge classification results and thus to compose

a multifarious overall picture (respectively data base) of the Wadden Sea ecosystem which can support the inter-disciplinary analysis of complex relationships and processes.

- The overview of the geomorphic and biogenic structural elements and habitats of the Wadden Sea ecosystem, their spatial arrangement and dynamics, seen from the perspective of satellite remote sensing using both optical and SAR sensors should be used to contribute to a holistic approach to monitor and further explore the eco-morphological evolution of the tidal system of the Wadden Sea and related tidal systems worldwide.

Author Contributions: H.F. and S.L. conceived and designed the basic project, managed the funding acquisition (WIMO) and provided resources. W.A. refined the project, conducted the research and investigation, performed the data collection and analysis and synthesized the data in the GIS. W.A. wrote the paper, which was commented on by H.F. and reviewed by S.L. and M.E. Validation of the data in the field were carried out by W.A. and H.F. M.E. was involved as external mentor and contributed to the financing.

Funding: This research was carried out as part of the project "Scientific Monitoring Concepts for the German Bight" (WIMO) funded by the Lower Saxony Ministry for the Environment, Energy and Climate Change and the Lower Saxony Ministry for Research and Culture (grant numbers VWZN2564., VWZN2869, VWZN2881). The APC was funded by DLR-MF.

Acknowledgments: The Ministries are highly acknowledged for the funding. We thank DLR for providing the TerraSAR-X data via project COA1075. We are grateful to Ursula Marschalk und Achim Roth (DLR) for their support in acquiring data, which had to be in sync with field campaigns, and also to the colleagues from the DLR Forschungsstelle Maritime Sicherheit, Bremen for the workplace, help and fruitful discussions. We also thank the Institute for Advanced Study (HWK) in Delmenhorst, especially Doris Meyerdierks and Verena Backer for the WIMO overall project management and the function of HWK as platform for discussions and workshops. In the WIMO subproject "Remote sensing", the cooperation with the colleagues from the University of Osnabrück (IGF), especially Richard Jung, the University of Hannover (IPI) with Alena Schmidt and the Senckenberg Institute in Wilhelmhaven with Ruggero Capperucci and Alexander Bartholomä gave insights into the possibilities of the different sensory systems and their pro and cons. We thank our colleagues for the good teamwork especially in the joint field campaigns and the many fruitful discussions. Equally we thank our colleagues from the projects DeMarine-1 and DeMarine-2, Martin Gade, Kerstin Stelzer, Gabriele Müller, Kai Eskildsen, and Jörn Kohlus and also the colleagues from the DLR, Andrey Pleskachevsky, Stephan Brusch and Wolfgang Rosenthal for close cooperation over many years. Thanks also to the reviewers for their advice which helped to improve the text. Personal thanks to Gerald Millat und Gregor Scheiffarth from the National Park Administration Lower Saxon Wadden Sea, whose support of our work was of particular importance and who were always willing to discuss or help.

Conflicts of Interest: The authors declare no conflict of interest. The founding sponsors had no role in the design of the study; in the collection, analyses, or interpretation of data; in the writing of the manuscript, and in the decision to publish the results.

References

1. Millat, G. *Entwicklung Eines Methodisch-Inhaltlichen Konzeptes zum Einsatz von Fernerkundungsdaten für ein Umweltmonitoring im Niedersächsischen Wattenmeer*; Schriftenreihe der Nationalparkverwaltung Niedersächsisches Wattenmeer: Wilhelmshaven, Germany, 1996; Volume 1, pp. 1–125.
2. Herlyn, M.; Millat, G. *Wissenschaftliche Begleituntersuchungen zur Aufbauphase des Miesmuschelmanagements im Nationalpark "Niedersächsisches Wattenmeer"*; Abschlussbericht der Niedersächsischen Wattenmeerstiftung; Wilhelmshaven, Germany, 2004, (unpublished data).
3. Herlyn, M. Quantitative assessment of intertidal blue mussel (*Mytilus edulis* L.) stocks: Combined methods of remote sensing, field investigation and sampling. *J. Sea Res.* **2005**, *53*, 243–253. [CrossRef]
4. Ringot, J.L. Erstellen eines Interpretationsschlüssels und Kartierung der Biotoptypen terrestrischer Bereiche des Nationalparks Niedersächsisches Wattenmeer auf der Basis des CIR-Bildfluges vom 21.08.1991. 1992/1993, (unpublished data).

5. Esselink, P.; Petersen, J.; Arens, S.; Bakker, J.P.; Bunje, J.; Dijkema, K.S.; Hecker, N.; Hellwig, U.; Jensen, A.-V.; Kers, A.S.; et al. Salt Marshes. Thematic Report No. 8. In *Quality Status Report 2009—Wadden Sea Ecosystem 25*; Marencic, H., Vlas, J., Eds.; Common Wadden Sea Secretariat, Trilateral Monitoring and Assessment Group: Wilhelmshaven, Germany, 2009.
6. Petersen, J.; Dassau, O.; Dauck, H.-P.; Janinhoff, N. Applied vegetation mapping of large-scale areas based on high resolution aerial photographs—A combined method of remote sensing, GIS and near comprehensive field verification. *Wadden Sea Ecosyst.* **2010**, *26*, 75–79.
7. Kolbe, K. Erfassung der Seegrasbestände im niedersächsischen Wattenmeer über visuelle Luftbildinterpretation—2008. *Küstengewässer und Ästuare* **2011**, *4*, 1–35.
8. Moreira, A.; Prats-Iraola, P.; Younis, M.; Krieger, G.; Hajnsek, I.; Papathanassiou, K.P. A tutorial on synthetic aperture radar. *IEEE Geosci. Remote Sens. Mag.* **2013**, *1*, 6–43. [CrossRef]
9. Stelzer, K.; Brockmann, C. Operationalisierung von Fernerkundungsmethoden fürs Wattenmeermonitoring (OFEW). Abschlussbericht, 2007. Available online: http://docplayer.org/7506004-Operationalisierung-von-fernerkundungsmethoden-fuer-das-wattenmeermonitoring-zusammenfassung.html (accessed on 27 April 2018).
10. Stelzer, K.; Geißler, J.; Gade, M.; Eskildsen, K.; Kohlus, J.; Farke, H.; Reimers, H.-C. *DeMarine Umwelt: Operationalisierung Mariner GMES-Dienste in Deutschland. Integration optischer und SAR Erdbeobachtungsdaten für das Wattenmeermonitoring*; Jahresbericht 2009–2010; Bundesamt für Seeschifffahrt und Hydrographie: Hamburg, Germany, 2010; pp. 37–55.
11. Müller, G.; Stelzer, K.; Smollich, S.; Gade, M.; Adolph, W.; Melchionna, S.; Kemme, L.; Geißler, J.; Millat, G.; Reimers, H.-C.; et al. Remotely sensing the German Wadden Sea—A new approach to address national and international environmental legislation. *Environ. Monit. Assess.* **2016**, *188*, 595. [CrossRef] [PubMed]
12. Winter, C.; Backer, V.; Adolph, W.; Bartholomä, A.; Becker, M.; Behr, D.; Callies, C.; Capperucci, R.; Ehlers, M.; Farke, H.; et al. *WIMO—Wissenschaftliche Monitoringkonzepte für die Deutsche Bucht*; Abschlussbericht; 2016; pp. 1–159. Available online: http://dx.doi.org/10.2314/gbv:860303926 (accessed on 05 July 2018). [CrossRef]
13. Winter, C. Monitoring concepts for an evaluation of marine environmental states in the German Bight. *Geo-Mar. Lett.* **2017**, *37*, 75–78. [CrossRef]
14. Gade, M.; Alpers, W.; Melsheimer, C.; Tanck, G. Classification of sediments on exposed tidal flats in the German Bight using multi-frequency radar data. *Remote Sens. Environ.* **2008**, *112*, 1603–1613. [CrossRef]
15. Jung, R.; Adolph, W.; Ehlers, M.; Farke, H. A multi-sensor approach for detecting the different land covers of tidal flats in the German Wadden Sea—A case study at Norderney. *Remote Sens. Environ.* **2015**, *170*, 188–202. [CrossRef]
16. Gade, M. A polarimetric radar view at exposed intertidal flats. In Proceedings of the 2016 IEEE International Geoscience and Remote Sensing Symposium (IGARSS), Beijing, China, 10–15 July 2016.
17. Jung, R. A Multi-Sensor Approach for Land Cover Classification and Monitoring of Tidal Flats in the German Wadden Sea. Ph.D. Dissertation, University of Osnabrueck, Osnabrueck, Germany, December 2015.
18. Wang, W.; Yang, X.; Liu, G.; Zhou, H.; Ma, W.; Yu, Y.; Li, Z. Random Forest Classification of Sediments on Exposed Intertidal Flats Using ALOS-2 Quad-Polarimetric SAR Data. *Int. Arch. Photogramm. Remote Sens. Spat. Inf. Sci.* **2016**, *8*, 1191–1194. [CrossRef]
19. Adolph, W.; Schückel, U.; Son, C.S.; Jung, R.; Bartholomä, A.; Ehlers, M.; Kröncke, I.; Lehner, S.; Farke, H. Monitoring spatiotemporal trends in intertidal bedforms of the German Wadden Sea in 2009–2015 with TerraSAR-X, including links with sediments and benthic macrofauna. *Geo-Mar. Lett.* **2017**, *37*, 79–91. [CrossRef]
20. Adolph, W.; Jung, R.; Schmidt, A.; Ehlers, M.; Heipke, C.; Bartholomä, A.; Farke, H. Integration of TerraSAR-X, RapidEye and airborne lidar for remote sensing of intertidal bedforms on the upper flats of Norderney (German Wadden Sea). *Geo-Mar. Lett.* **2017**, *37*, 193–205. [CrossRef]
21. Geng, X.-M.; Li, X.-M.; Velotto, D.; Chen, K.-S. Study of the polarimetric characteristics of mud flats in an intertidal zone using C- and X-band spaceborne SAR data. *Remote Sens. Environ.* **2016**, *176*, 56–68. [CrossRef]
22. Wang, W.; Gade, M. A new SAR classification scheme for sediments on intertidal flats based on multi-frequency polarimetric SAR imagery. *Int. Arch. Photogramm. Remote Sens. Spat. Inf. Sci.* **2017**, *XLII-3/W2*, 223–228. [CrossRef]
23. Gade, M.; Wang, W.; Kemme, L. On the imaging of exposed intertidal flats by single- and dual-co-polarization Synthetic Aperture Radar. *Remote Sens. Environ.* **2018**, *205*, 315–328. [CrossRef]

24. Albertz, J. *Einführung in die Fernerkundung. Grundlagen der Interpretation von Luft- und Satellitenbildern*, 4th ed.; Wissenschaftliche Buchgesellschaft: Darmstadt, Germany, 2009; ISBN 978-3-534-23150-8.
25. Eitner, V.; Kaiser, R.; Niemeyer, H.D. Nearshore sediment transport processes due to moderate hydrodynamic conditions. In *Geology of Siliciclastic Shelf Seas*; de Batist, M., Jacobs, P., Eds.; Geological Society: London, UK, 1996; pp. 267–288.
26. Hayes, M.O. Barrier islands morphology as a function of tidal and wave regime. In *Barrier Islands*; Leatherman, S.P., Ed.; Academic Press: New York, NY, USA, 1979; pp. 1–28.
27. Fritz, T.; Eineder, M. TerraSAR-X Ground Segment Basic Product Specification Document. Available online: http://sss.terrasar-x.dlr.de/docs/TX-GS-DD-3302.pdf (accessed on 27 April 2018).
28. Airbus Defence & Space. Radiometric Calibration of TerraSAR-X Data. Beta Naught and Sigma Naught Coefficient Calculation. TSXX-ITD-TN-0049-radiometric_calculations_I3.00.doc. Available online: https://dep1doc.gfz-potsdam.de/attachments/download/365/r465_9_tsx-x-itd-tn-0049-radiometric_calculations_i3.00.pdf (accessed on 27 April 2018).
29. Haralick, R.M.; Shanmugam, K.; Dinstein, I. Textural Features for Image Classification. *IEEE Trans. Syst. Man. Cybern.* **1973**, *3*, 610–621. [CrossRef]
30. Farke, H. *DeMarine-Umwelt: TP 4—Integration Optischer und SAR Beobachtungsdaten für das Wattenmeermonitoring*; Schlussbericht; 2011. Available online: http://dx.doi.org/10.2314/gbv:722405367 (accessed on 05 July 2018). [CrossRef]
31. NLPV. Monitoring Data: Aerial Mapping for Annual Mussel Monitoring. Available online: http://www.nationalpark-wattenmeer.de/nds/service/publikationen/1130_muschelwildbänke-von-borkum-bis-cuxhaven-gis-daten (accessed on 26 April 2018).
32. Deutscher Wetterdienst (DWD). Available online: www.dwd.de/DE/presse/pressemitteilungen/DE/2014/20140730_Deutschlandwetter_Juli_2014.html (accessed on 28 April 2018).
33. UnwetterZentrale. Available online: http://www.unwetterzentrale.de/uwz/955.html (accessed on 28 April 2018).
34. Lee, H.; Chae, H.; Cho, S.-J. Radar Backscattering of Intertidal Mudflats Observed by Radarsat-1 SAR Images and Ground-Based Scatterometer Experiments. *IEEE Trans. Geosci. Remote Sens.* **2011**, *49*, 1701–1711. [CrossRef]
35. Choe, B.-H.; Kim, D.-J.; Hwang, J.-H.; Oh, Y.; Moon, W.M. Detection of oyster habitat in tidal flats using multi-frequency polarimetric SAR data. *Estuar. Coast. Shelf Sci.* **2012**, *97*, 28–37. [CrossRef]
36. Cheng, T.-Y.; Yamaguchi, Y.; Chen, K.-S.; Lee, J.-S.; Cui, Y. Sandbank and Oyster Farm Monitoring with Multi-Temporal Polarimetric SAR Data Using Four-Component Scattering Power Decomposition. *IEICE Trans. Commun.* **2013**, *96*, 2573–2579. [CrossRef]
37. Gade, M.; Melchionna, S.; Kemme, L. Analyses of multi-year synthetic aperture radar imagery of dry-fallen intertidal flats. *Int. Arch. Photogramm. Remote Sens. Spat. Inf. Sci.* **2015**, *XL-7/W3*, 941–947. [CrossRef]
38. Gade, M.; Melchionna, S. Joint use of multiple Synthetic Aperture Radar imagery for the detection of bivalve beds and morphological changes on intertidal flats. *Estuar. Coast. Shelf Sci.* **2016**, *171*, 1–10. [CrossRef]
39. Park, S.-E.; Moon, W.M.; Kim, D.-J. Estimation of Surface Roughness Parameter in Intertidal Mudflat Using Airborne Polarimetric SAR Data. *IEEE Trans. Geosci. Remote Sens.* **2009**, *47*, 1022–1031. [CrossRef]
40. Ryu, J.-H.; Eom, J.A.; Choi, J.-K. Application of airborne remote sensing to the surface sediment classification in a tidal flat. In Proceedings of the IGARSS 2010: 2010 IEEE International Geoscience and Remote Sensing Symposium, Honolulu, HI, USA, 25–30 July 2010; pp. 942–945. [CrossRef]
41. Eom, J.A.; Choi, J.-K.; Ryu, J.-H.; Woo, H.J.; Won, J.-S.; Jang, S. Tidal channel distribution in relation to surface sedimentary facies based on remotely sensed data. *Geosci. J.* **2012**, *16*, 127–137. [CrossRef]
42. Choi, J.-K.; Eom, J.A.; Ryu, J.-H. Spatial relationships between surface sedimentary facies distribution and topography using remotely sensed data: Example from the Ganghwa tidal flat, Korea. *Mar. Geol.* **2011**, *280*, 205–211. [CrossRef]
43. Mason, D.C.; Scott, T.R.; Dance, S.L. Remote sensing of intertidal morphological change in Morecambe Bay, U.K., between 1991 and 2007. *Estuar. Coast. Shelf Sci.* **2010**, *87*, 487–496. [CrossRef]
44. Wiehle, S.; Lehner, S.; Pleskachevsky, A. Waterline detection and monitoring in the German Wadden Sea using high resolution satellite-based Radar measurements. *Int. Arch. Photogramm. Remote Sens. Spat. Inf. Sci.* **2015**, *XL-7/W3*, 1029–1033. [CrossRef]

45. Klonus, S.; Rosso, P.; Ehlers, M. Image Fusion of High Resolution TerraSAR-X and Multispectral Electro-Optical Data for Improved Spatial Resolution. In *Remote Sensing—New Challenges of High Resolution*; Jürgens, C., Ed.; EARsel Joint Workshop: Bochum, Germany, 2008; pp. 249–264. ISBN 978-3-925143-79-3.
46. Klonus, S.; Ehlers, M. Additional Benefit of Image Fusion Method from Combined High Resolution TerraSAR-X and Multispectral SPOT Data for Classification. In Proceedings of the 29th Annual EARSeL Symposium, Chania, Kreta, 15–18 June 2009.
47. Rosso, P.H.; Michel, U.; Civco, D.L.; Ehlers, M.; Klonus, S. Interpretability of TerraSAR-X fused data. In Proceedings of the SPIE Europe Remote Sensing, Berlin, Germany, 31 August 2009. [CrossRef]
48. Metz, A.; Schmitt, A.; Esch, T.; Reinartz, P.; Klonus, S.; Ehlers, M. Synergetic use of TerraSAR-X and Radarsat-2 time series data for identification and characterization of grassland types—A case study in Southern Bavaria, Germany. In Proceedings of the 2012 IEEE International Geoscience and Remote Sensing Symposium (IGARSS), Munich, Germany, 22–27 July 2012; pp. 3560–3563. [CrossRef]
49. Van der Wal, D.; Herman, P.M.J. Regression-based synergy of optical, shortwave infrared and microwave remote sensing for monitoring the grain-size of intertidal sediments. *Remote Sens. Environ.* **2007**, *111*, 89–106. [CrossRef]
50. Gade, M.; Melchionna, S.; Stelzer, K.; Kohlus, J. Multi-frequency SAR data help improving the monitoring of intertidal flats on the German North Sea coast. *Estuar. Coast. Shelf Sci.* **2014**, *140*, 32–42. [CrossRef]
51. Luus, F.P.S.; Salmon, B.P.; van den Bergh, F.; Maharaj, B.T.J. Multiview Deep Learning for Land-Use Classification. *IEEE Geosci. Remote Sens. Lett.* **2015**, *12*, 2448–2452. [CrossRef]
52. Cheng, G.; Yang, C.; Yao, X.; Guo, L.; Han, J. When Deep Learning Meets Metric Learning: Remote Sensing Image Scene Classification via Learning Discriminative CNNs. *IEEE Trans. Geosci. Remote Sens.* **2018**, *99*, 2811–2821. [CrossRef]